

# Approach to determine wind loads on small heliostats<sup>☆</sup>

Andreas Pfahl

German Aerospace Center (DLR), Institute of Solar Research, Concentrating Solar Technologies (CST), Im Langenbroich 13, 52428 Jülich, Germany

## ARTICLE INFO

### Keywords:

Solar Tower Plants  
Heliostats  
Size  
Wind Forecast  
Wind Loads

## ABSTRACT

Due to changing boundary conditions like reduced controller cost and the need for higher flux densities, smaller heliostats have become more and more important in recent decades. The methods for determining heliostat wind loads were initially developed for the larger heliostats common at the time. For smaller heliostats, it is important to choose suitable methods for the individual steps of wind load determination and, if necessary, to adapt them to the lower height. These steps involve determining the maximum wind speeds, the turbulence spectra, the pressure distribution time series, the dynamic amplification, and the wind load spectra.

## 1. Introduction

In recent years, the cost optimum of heliostats has shifted towards smaller mirror areas. While several studies from a decade ago stated sizes of around 50 m<sup>2</sup> [6,24,25], the preliminary results of the latest study for applications of 565 °C or higher are between 5 and 15 m<sup>2</sup> [9]. The disadvantage of such small heliostats is the larger number of controls and cabling required for the heliostat field. However, the rapid decline in the cost of electronic components, including PV and battery systems, has made this disadvantage less significant. Small heliostats have the advantage of a lower weight per mirror area. That is because the mirror surface only increases quadratically with the side length, while the volume and thus the weight of the structural elements increases cubically [16]. Further advantages of smaller heliostats are their lower height, which is associated with lower wind speeds, suitability for large-scale production [11], and better transportability. With the use of smaller solar tower systems for solar fuel production, another point has to be considered: the high required flux densities of up to 3 MW/m<sup>2</sup> can only be achieved economically with heliostats with very high optical efficiency. In smaller systems, however, large heliostats have a large astigmatism error [28]. This would lead to a very high number of required heliostats and thus to high costs as shown for a sample case by Pfahl and Dohmen [23].

The main load on heliostats is due to wind. Wind loads are usually determined by means of wind tunnel tests. Emes et al. [7] have provided a comprehensive overview on this. In wind tunnel tests, it is not only important that the wind speed in the wind tunnel increases with height (wind profile) as in reality, but also that the turbulence is modeled

correctly. Both depend on the surrounding of the heliostat field. To avoid having to model the environment for every specific case, possible environments for buildings and larger heliostats can be divided into categories. Boundary layer wind tunnel providers have the appropriate turbulence and wind profile generators available for these categories. Since solar fields are usually erected in unbuilt surroundings, the “open country” category is usually used for heliostats. For this category, there is some literature available with wind load coefficients for heliostats (e. g. [18,22,27]), so the static wind loads can be roughly determined even without own wind load tests, provided that the geometry of the heliostat matches that of the literature. However, this procedure is not suitable for small heliostats. On the one hand, because previous literature values generally apply to larger heliostats with the corresponding turbulence intensity for higher heights. On the other hand, the gradients of the wind speed and turbulence intensity profiles increase significantly towards the ground. Therefore, inaccuracies in the modeling of the ground roughness, as they are given with the usual use of only a few ground categories, lead to larger errors.

For smaller heliostats, precise wind speed profiles and turbulence spectra at heliostat height would therefore have to be measured at the particular site in order to be able to develop and build suitable wind tunnel set-ups to simulate the ground roughness. This means a considerable additional effort. It would therefore be desirable to be able to calculate the wind loads. Li et al. [17] presented an approach using Large Eddy Simulations (LES).

A disadvantage of conventional wind tunnel tests and also of pure LES calculations is that the dynamic behavior and therefore also the dynamic wind loads cannot be simulated with the rigid heliostat models

<sup>☆</sup> This article is part of a special issue entitled: ‘Heliostats’ published in Solar Energy.

E-mail address: [Andreas.Pfahl@dlr.de](mailto:Andreas.Pfahl@dlr.de).

usually used. With aeroelastic wind tunnel models it is possible, but very expensive and still inaccurate. Dynamic wind loads can be calculated using the fluid–structure interaction method (FSI), but this is computationally very extensive. A cost-effective method was presented by Gong et al. [10]. They determined the pressure distribution time series in the wind tunnel and used them in a transient finite element analysis (FEA) simulation. Blum et al. [4] have developed a method to reduce the computational effort of this approach by using a coarser model to determine the time periods of maximum deformation first and applying the precise model only to these time periods.

In addition to the maximum loads, the number of load cycles is also required for the dimensioning of heliostats in order to exclude failure due to fatigue. The method proposed by [20] can be used for this purpose.

In this contribution, it is presented which of these methods should be applied and in which way to determine the wind loads on small heliostats.

## 2. Wind speed and direction

The maximum wind speeds are the basis for any wind load determination. A distinction must be made between the maximum wind speed while the heliostat is operating or moving into the stow position and the one that is expected at the specific site and at which the heliostat is in the horizontally aligned stow position.

### 2.1. Maximum wind speed while heliostat is moving

During operation, the mirror is usually not aligned horizontally, which means that it has a much larger area exposed to the wind than in the stow position. To reduce costs, a maximum operating wind speed is therefore defined that is significantly below the maximum wind speed of the location. However, this means that the plant loses yield at times when operation is not possible due to high wind speeds. In order to determine the most cost-efficient maximum operating wind speed, the resulting monetary loss must be weighed against the savings on heliostats resulting from the reduced wind loads.

It must be considered that the heliostat needs a certain time to reach the stow position. It is therefore not sufficient to dimension the heliostat according to the maximum operating wind speed, as the wind can increase till the stow position is reached. The maximum wind speed while the heliostat is moving can therefore be significantly higher than the maximum operating wind speed which leads to much higher wind loads as the wind speed factors quadratically into the calculation of the wind loads. For an operational wind speed of 10 m/s and a safety margin of 8 m/s e.g., three times (!) higher wind loads have to be considered.

However, if it were possible to forecast the exceeding of the maximum operating wind speed, the heliostat could be moved to the stow position in time and no higher maximum wind speed would have to be assumed. The time needed to get from vertical to horizontal mirror orientation is typically a few minutes. Anemometers, for example, could be placed around the heliostat field or on the prevailing wind side of the heliostat field at least for sites with a predominant wind direction. But they would have to be at a sufficient distance so that the heliostats can move to the stow position early enough. They would also have to be sufficiently dense. As this would be very expensive and as the land where the anemometers would have to be installed normally has other owners, this approach does not seem practicable. But a possible approach is to use a wind lidar to scan the surroundings regarding wind speed at a distance of up to several kilometers and thus be able to warn of excessive wind speeds in time. This approach is described by Conseil [5] and Ibrahim [15]. Another possibility is to use weather forecast models that can be refined for the specific site using local wind measurements and AI. With it, warnings of weather patterns with possibly too high wind speeds could be provided [1].

One way of reducing the design wind loads is to move the heliostats,

which are unfavorably aligned and located at the edge and not in the strong lee of other heliostats, into the safety position at lower wind speeds or at least into an alignment that leads to lower wind loads. This does result in a slight loss of yield. However, as only a few heliostats are affected, this loss is relatively small. The efficiency of this approach could be increased by monitoring the edge areas of the heliostat field to determine which heliostats are particularly affected by the current wind conditions. The monitoring could be achieved using sensors on the heliostats or, probably more simply, using cameras installed on the tower. The sensors or cameras would detect the strength of fluctuations of the mirror, which would allow to conclude on the wind load. For that, a relationship between wind load and surface fluctuations would need to be developed. Over time, this could be used to determine which field positions are particularly critical for which wind direction, heliostat alignment and wind speed. With AI support, this knowledge could be gained in a shorter time. Over time, this would make it possible to dispense with the sensors or cameras, including for other similar heliostat fields.

### 2.2. Maximum wind speed while heliostat is in stow position

Wind standards with wind speed maps are available for many countries. They provide the maximum wind speeds at a height of 10 m for the various regions of the country. The wind profile and thus the maximum wind speed at heliostat height can be calculated using the terrain category of the surrounding of the site. However, it can be determined more precisely with anemometer measurements on site, which is particularly relevant for small heliostats, as the wind profile, as already mentioned in the introduction, shows an increasing gradient with lower altitude. When taking measurements, it is important to ensure that the wind speed is sufficiently high so that the wind profile is not distorted by thermal effects.

In case the surroundings of the heliostat field site are not uniform, the wind direction must also be considered. If the highest wind speeds can only occur from one prevailing wind direction, wind measurements with this wind direction can be used. Otherwise, all possible wind directions must be considered and the one with the most unfavorable wind profile has to be taken into account.

If no wind speed maps are available, historical wind data can be used. This can be analyzed using extreme value statistics to calculate the maximum wind speed ([19], Appendix A). The main wind direction can also be determined from this data, if not otherwise known.

## 3. Turbulence

One advantage of small heliostats is the lower height with the associated lower wind speeds. However, the intensity of the turbulence increases with reduced height. This must be considered especially for load cases that are strongly affected by turbulence i.e. orientations with a high ratio of peak load to mean load. These are in particular the moment about a horizontal axis ( $M_{Hy}$  or  $M_{Hx}$ ) with horizontal mirror alignment and the moment about the vertical axis ( $M_z$ ) with vertical mirror and flow parallel to the mirror surface. This is explained in the following for  $M_{Hy}$ .

$M_{Hy}$  is calculated according to Peterka and Derickson [18] using the following formula:

$$M_{Hy} = c_{MHy} \frac{\rho}{2} v_H^2 A h \quad (1)$$

With  $c_{MHy}$  for the wind load coefficient of the hinge moment,  $\rho$  for the air density,  $v_H$  the mean wind speed at elevation axis height  $H$ ,  $A$  the mirror area, and  $h$  the chord length of the mirror. This formula reflects the fact that the hinge moment increases proportionally with the individual factors with the exception of the wind speed which is squared. The dependency of the wind speed on height can be calculated using the logarithmic law [18]:

$$v_H = v_{10m} \frac{\ln \frac{H}{z_0}}{\ln \frac{10m}{z_0}} \quad (2)$$

With  $v_{10m}$  for the mean wind speed at 10 m height and  $z_0$  for the ground roughness of the surrounding which is typically 0.03 m for the terrain category “open country”.

All in all, the hinge moment would increase with the mirror area as given by the blue dashed graph of Fig. 1. Here, the hinge moment is normalized to an area of 100 m<sup>2</sup>. For the heliostat height, half the square root of the mirror surface  $A$  is assumed.

But the height also impacts the turbulence intensity and thus the wind load coefficient. By Pfahl [19] the following dependency of the hinge moment on the vertical turbulence intensity  $I_w$  was determined:

$$c_{MHy} = 1.45I_w^2 + 0.48I_w^2 \quad (3)$$

The vertical turbulence intensity can be calculated from the longitudinal turbulence intensity  $I_u$  by the standard ESDU 85020 [8]:

$$I_w = 0.55I_u \quad (4)$$

Holmes ([13], eq. (3.18)) gives the following relationship for the height dependency of the longitudinal turbulence intensity near the ground:

$$I_u = \frac{1}{\ln \frac{H}{z_0}} \quad (5)$$

This results in the orange continuous graph of Fig. 1 which shows the overall impact of the wind speed and the wind load coefficients on the hinge moment, which both change with height. If the impact of the turbulence is not taken into account, the load for a 10 m<sup>2</sup> mirror, for example, would be assumed 26 % too low (difference between the solid and dashed graphs). This difference is smaller for larger heliostats. For 50 m<sup>2</sup>, for example, the difference is only 8 %. This shows that the impact of turbulence on the wind load coefficients must be considered, especially for small heliostats.

The turbulence intensity at site can be determined by classifying the surrounding into the corresponding terrain category. However, especially for low heights, the turbulence intensity is also strongly affected by specific terrain structures that cannot be covered by the terrain categories. For this reason and due to the stronger gradient of the turbulence intensity profile near the ground, a measurement directly on site leads to significantly more accurate values, especially for smaller heliostats.

In order to model the turbulence as realistically as possible, not only the turbulence intensity but also the turbulence energy spectra should be determined, preferably for all three spatial directions. For this, the wind

speed time series must be measured with 3D anemometers. Pfahl [19] had shown that for the stow position the hinge moment  $M_{Hy}$  and the vertical force  $F_z$  do not depend on the shape of the spectra, but solely on the turbulence intensity, i.e. the peak frequency is of minor relevance which is approximately corresponding to the dominant scale of turbulent eddies. For the determination of the dynamic forces, however, it is of relevance, which means that in the simulations a good match of the turbulence energy spectra should be aimed for nevertheless.

#### 4. Pressure distribution time series

The simulations to determine the pressure distribution time series can be performed using a wind tunnel or CFD. They could also be measured directly on site using a heliostat equipped with pressure sensors. However, this would be a significant effort, also because it would mean waiting for a sufficiently high wind speed from a suitable direction.

A problem with measurements in the wind tunnel is that relevant low frequencies cannot be generated, particularly with small heliostats. The reason is that only vortices up to the size of the wind tunnel can be generated, so frequencies caused by larger vortices cannot occur, cf. Fig. 2 [19]. Since a relatively large model scale must be chosen for small heliostats in order to be able to model the structure of the heliostat and the wind speed and turbulence profile at heliostat height accurately, a relatively large part of the spectrum cannot be simulated. Although there are proposals to compensate for this effect [2], this leads to an increase in measurement inaccuracy. A further difficulty is that turbulence generating devices suitable for the spectra and the unusually large model scale have to be developed, which means considerable additional costs.

For these reasons, it would be desirable, especially for smaller heliostats, to determine the pressure distribution time series using CFD. Li et al. [17] have presented a promising method. It involves a Large Eddy Simulation (LES) in which the turbulence is generated by a spectral method called PRFG<sup>3</sup> matching turbulence spectra and length scales at real scale. However, a validation of the method by full-scale measurements is still lacking.

#### 5. Dynamic amplification

In principle, the dynamic loads could be determined directly with the LES calculations if the movements of the heliostat were made possible with the Fluid-Structure Interaction (FSI) method. However, this is computationally very time-consuming and not necessary, as the movements of the heliostat are small in relation to the sizes of the relevant turbulence structures. Therefore, the pressure distribution time series

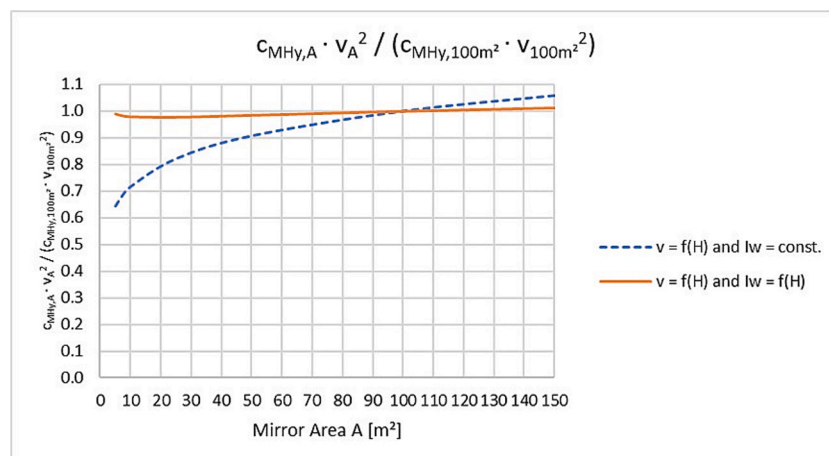


Fig. 1. Impact of wind speed profile only on hinge moment (blue dashed graph) and including also turbulence intensity profile (orange continuous graph).

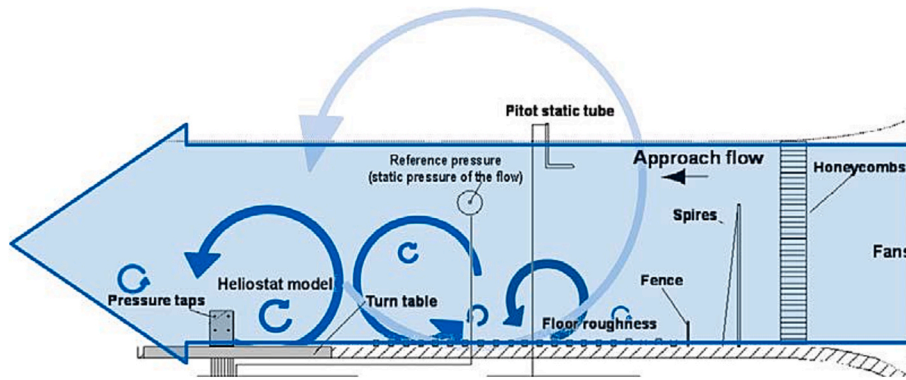


Fig. 2. Size restriction of wind tunnel that limits the size of vortices that can be simulated [19].

and the resulting movement of the heliostat can be determined separately. It is not possible to determine the dynamic loads in outdoor tests, as resonance effects depend on the excitation frequency and this in turn depends on the wind speed. It would therefore be necessary to have the maximum possible wind speeds available for the measurements, which is obviously practically impossible.

The pressure distribution time series, on the other hand, can be obtained at lower wind speeds. This is because the pressure distribution time series of higher speeds can be calculated from these, as it can be assumed that the pressure distribution on the mirror surface increases in the same way as the dynamic pressure with the second power of the wind speed (at least for sufficiently high wind speeds with negligible impact of thermal effects).

To determine the dynamic amplification, the pressure distribution time series can be applied to the structural-mechanical heliostat model in a transient FEA simulation. Components that are not relevant for the deformations, such as the motors, can be removed for simplification, but must be represented by a corresponding mass point. In general, a simulation duration of 10 min (based on an average outdoor wind speed) is considered sufficient, as it has been shown for many locations that all excitation frequencies resulting from the ground roughness of the surrounding area occur during this period [14]. Frequencies that result from temperature differences and are caused, for example, by the change of day and night or seasons are significantly lower and have almost no impact on dynamic effects (besides their impact on the maximum wind speed that has to be considered).

But even with all permissible model simplifications and the limitation to 10 min, a transient calculation is still very time-consuming, as a very short time step corresponding to the highest resonance frequency to be considered is required to calculate the stresses. Blum et al. [4] have therefore developed a method that can significantly reduce the calculation times. This method takes advantage of the fact that a much simpler model is sufficient for calculating the deformations of the heliostat. With this model, one or a few time periods of largest

deformations are determined (Fig. 3). These time periods are not necessarily the time periods of highest wind speeds as lower wind speeds at critical frequencies can lead to even higher dynamic loads. A more detailed model is then used to simulate only this one or these few critical time periods in order to calculate the maximum stresses. The Mode Superposition Method (MSUP) is applied for the calculations, which already leads to a considerable reduction in calculation time. For the simplified model, the considered modes and the fineness of the grid are reduced to such an extent that a sufficiently accurate calculation of the deformations is still possible. This was the case for an amount of considered modes reduced from 30 to 10 and a finite element size increased by a factor of 6. By this, the computational time was reduced by a factor of 4.5 [3]. The results are the maximum stresses which can be validated by stress-strain data of discrete components gained by full-scale measurements.

With their method, Blum et al. [4] were able to determine a dynamic amplification factor of the maximum stresses in the structure of 1.4 for a 2 m<sup>2</sup> heliostat in the stow position. By Pfahl et al. [21], a ratio of the static and the dynamic maximum hinge moment of 2.0 is given for an 8 m<sup>2</sup> heliostat in stow. For the same heliostat at 5°, 10°, and 20° elevation angles, Vasquez [26] calculated dynamic amplification factors of the hinge moment of 2.3, 2.2, and 2.8 respectively. This confirms the general trend for smaller heliostats to have lower amplification factors than larger ones, which is another advantage.

## 6. Fatigue

For the reliable design of heliostats, it is not only important to ensure that the maximum peak loads are not exceeded during the service life, but also that individual components do not fatigue due to alternating loads and thus fail. In order to be able to prove this through tests or calculations, the number of load cycles must be known. Not only the highest wind loads, which occur relatively rarely, are relevant for determining fatigue, but also lower loads, especially as they occur much

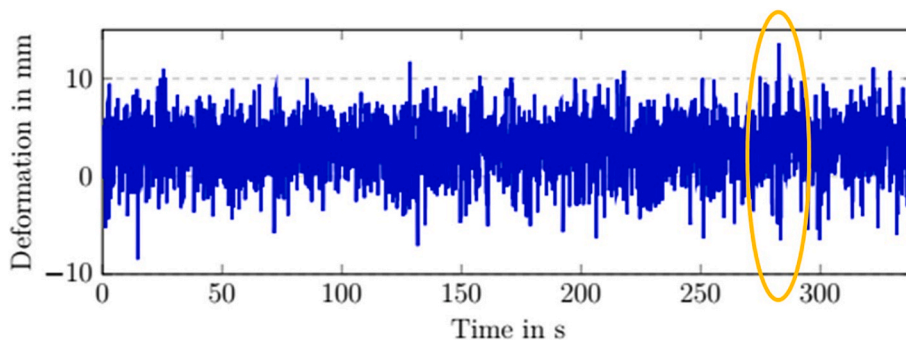


Fig. 3. Time period of largest deformation [12].

more frequently. Therefore, the number of load cycles for each load level must be known. The total number of load cycles in relation to the individual load levels forms the so-called load spectrum.

Pfahl [20] has proposed a method for estimating the load spectrum for heliostats in a simple way. It is based on the wind load spectra for buildings given in Eurocode EN 1991 1–4, Fig. 4. However, since small heliostats are significantly lower than the buildings on which this standard is based, and because the frequency of wind fluctuations increases with lower heights, it is particularly important to adjust the number of load cycles to the height of small heliostats.

Especially for the stow position this is relevant, since the vertical velocity component of the vortices is decisive here. The size of the relevant vortices which make a major contribution to the vertical component  $D_{vortices}$  is in turn linearly dependent on the height of the mirror surface, as shown in ([19], Fig. 71):

$$D_{vortices} \propto H \quad (6)$$

According to Pfahl ([19], eq. (B12)), the following applies to the main excitation frequency  $f_{excitation}$ :

$$f_{excitation} \propto \frac{1}{D_{vortices}} \quad (7)$$

So, all in all it follows:

$$f_{excitation} \propto \frac{1}{H} \quad (8)$$

Thus, assuming that EN 1991 1–4, B.3 applies to heights of 10 m, this results in a factor of  $10/H$  by which the number of load cycles must be adjusted.

## 7. Summary and Outlook

To determine the dynamic wind loads on small heliostats, it is proposed to combine the following methods with adjustments regarding the low height:

1. Maximum wind speeds
  - a. Moving to stow: Maximum allowable wind speed determined by cost optimization of energy yield and heliostat costs; use of AI-refined short-term wind forecasts (nowcasting) and/or wind lidar.
  - b. Stow: Wind speed maps from standards; wind profile from local measurements.
2. Turbulence: Measurement of turbulence-energy spectra at heliostat height using 3D anemometers on site.
3. Pressure distribution time series: Generated by Large Eddy Simulations (LES) or wind tunnel tests with turbulence generation elements developed for measured spectra.
4. Dynamic amplification: Calculated by transient FEA simulations with MSUP and limitation to the critical time periods determined by a simplified model.
5. Fatigue: Determination of load spectra based on Eurocode EN 1991 considering the increased number of load cycles for lower heights.

This procedure is to be validated by field measurements of the dynamic loads. It is not possible to measure at the maximum possible wind speeds. However, it can be assumed with a high degree of probability that if the method provides realistic results for several lower wind speed levels, this should also be the case for higher wind speeds.

Potential to further simplify the procedure is seen by using AI especially for the FEA method to determine the pressure distribution time series. For to shorten the needed calculated time period of the dynamic amplification, extreme value statistics may be applied which would mean, that also all other measurements and calculations could be reduced to the same shorter time period.

Declaration of generative AI and AI-assisted technologies.

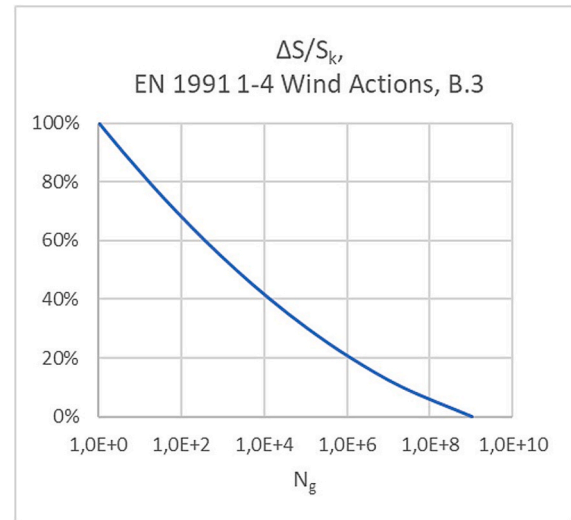


Fig. 4. Wind-induced fatigue cycle counts for buildings (Eurocode EN 1991 1–4). The loads are given in percentage of the maximum peak wind load event that occurs once within 50 years.

The author used DeepL in order to improve language only. The author reviewed all and takes full responsibility for the content of the publication.

## CRedit authorship contribution statement

**Andreas Pfahl:** Writing – review & editing, Writing – original draft, Visualization, Resources, Methodology, Investigation, Formal analysis, Data curation, Conceptualization.

## Acknowledgements

The author thanks the German Aerospace Center (DLR) for financing the development of this approach and the reviewers for improving the manuscript in many details.

## References

- [1] Arkipoff, I., 2024. “Overcoming weather challenges in PV trackers systems,” in: “Powering through: Tactics for weather-ready solar energy production,” Vaisala Webinar, <https://www.vaisala.com/en/events/webinars/1p/powering-through-solar>.
- [2] Banks, D., Guha, T.K., Fewless, Y.J., 2015. “Measuring peak wind loads on solar power assemblies,” The 14th International Conference on Wind Engineering, Porto Alegre, Brazil, 21–26 June 2015, <https://cppwind.com/wp-content/uploads/2020/12/A-hybrid-method-of-generating-realistic-full-scale-time-series-of-wind-loads-from-large-scale-wind-tunnel-studies-Application-to-solar-arrays-BanksGuhaFewless-2015.pdf>.
- [3] Blum, J., 2024. “Dynamische Auslegung eines Heliostaten unter Berücksichtigung der fluktuierenden Windlasten mittels FEM-Simulation,” Bachelor thesis, University of Applied Sciences Cologne and German Aerospace Center (DLR), <https://elib.dlr.de/208102/1/BachelorarbeitBlumJustus11149669.pdf>.
- [4] J. Blum, A. Helmer, A. Pfahl, “Dynamic Wind Loading of Heliostats: efficient simulation of resonance effects for heliostat cost-optimization,” SolarPACES Conference 2024, Italy, Oct, Rome, 2024, pp. 8–11.
- [5] Conseil, R., 2024. “Measuring the unpredictable with the Vaisala WindCube Scan,” Workshop Minute Scale Forecasting for the Weather Driven Energy System, DTU Risø Campus, 10–11 April 2024, [https://iea-wind.org/wp-content/uploads/2024/06/15\\_Vaisala\\_Measuring-the-unpredictable-11042024-DTU\\_Robin\\_Conseil.pdf](https://iea-wind.org/wp-content/uploads/2024/06/15_Vaisala_Measuring-the-unpredictable-11042024-DTU_Robin_Conseil.pdf).
- [6] Cordes, S., Prošinečki, T.C., Wieghardt, K., 2012. “An approach to competitive heliostat fields,” In: 18th annual SolarPACES symposium. 2012. Marrakesh.
- [7] M. Emes, A. Jafari, A. Pfahl, J. Coventry, M. Arjomandi, A Review of static and dynamic heliostat wind loads, Sol. Energy 225 (2021) 60–82, <https://doi.org/10.1016/j.solener.2021.07.014>.
- [8] ESDU 85020, 1985. “Characteristics of Atmospheric Turbulence Near the Ground, Part II: Single Point Data for Strong Winds (Neutral Atmosphere),” London, England, paragraph 4.2, equation (4.5).
- [9] A. Gamil, A. Zolan, A. Chad, G. Zhu, K. Armijo, “Techno-economic Analysis on Optimum Size of Heliostat for High Temperature Applications,” SolarPACES Conference 2024, Italy, Oct, Rome, 2024, pp. 8–11.

- [10] Gong, B., Li, Z., Wang, Z., Wang, Y., 2012. "Wind Induced Dynamic Response of Heliostat," *Renewable Energy*, 38-1, February 2012, 206-213, <https://doi.org/10.1016/j.renene.2011.07.025>.
- [11] B. Gross, "Beyond CSP—A Trillion Dollar Opportunity," *Plenary Presentation at SolarPACES 2020 Conference, online event, Sept. 28–Oct (2020) 2*.
- [12] Helmer, A.T., 2024. "Calculation of Dynamic Wind Loads on Heliostats Using FEM and Multibody Dynamics," Master Thesis, DLR, University of Applied Sciences Düsseldorf, [https://elib.dlr.de/208093/1/MscThesisHelmerFinal\\_signed.pdf](https://elib.dlr.de/208093/1/MscThesisHelmerFinal_signed.pdf).
- [13] J.D. Holmes, *Wind Loading of Structures*, 2nd edition, Taylor & Francis, New York, USA, 2007 <http://ndl.ethernet.edu.et/bitstream/123456789/12801/1/Wind%20Loading%20of%20Structures%202007.pdf>.
- [14] I. Van der Hoven, Power Spectrum of Horizontal wind speed in the frequency range from 0.0007 to 900 cycles per hour, *J. Meteorol.* 14 (1957) 160–164.
- [15] Ibrahim, J., 2024. "RAYGEN" in: "Powering through: Tactics for weather-ready solar energy production," Vaisala Webinar, <https://www.vaisala.com/en/events/webinars/lp/powering-through-solar>.
- [16] G.J. Kolb, S.A. Jones, M.W. Donnelly, D. Gorman, R. Thomas, R. Davenport, R. Lumia, "Heliostat Cost Reduction Study," SANDIA Report SAND2007-3293, Albuquerque, New Mexico, USA, 2007.
- [17] Li, W., Yang, F., Niu, H., Patruno, L., Hua, X., 2024. "Wind loads on heliostat tracker: A LES study on the role of geometrical details and the characteristics of near-ground turbulence," *Solar Energy*, 284, December 2024, 113041, <https://doi.org/10.1016/j.solener.2024.113041>.
- [18] Peterka, J.A., Derickson, R.G., 1992, "Wind Load Design Methods for Ground-Based Heliostats and Parabolic Dish Collectors," Tech. Rep. SAND92-7009, Sandia National Laboratories, Springfield, USA. <https://www.osti.gov/servlets/purl/7105290>.
- [19] Pfahl, A., 2018. "Wind Loads on Heliostats and Photovoltaic Trackers," PhD Thesis, DLR, TU Eindhoven, [https://pure.tue.nl/ws/files/99010995/20180621\\_Pfahl.pdf](https://pure.tue.nl/ws/files/99010995/20180621_Pfahl.pdf).
- [20] Pfahl, A., 2024. "Heliostat Fatigue Loads: Proposal for Estimation of Wind Load Collectives," *SolarPACES Conference Proceedings*, 2, Jul. 2024. DOI:<https://doi.org/10.52825/solarpaces.v2i.911>.
- [21] Pfahl, A., Blume, K., Hanrieder, N., Uhlig, R., 2020. "MAHWIN – Teilvorhaben Winddatenanalyse, Freilandmessungen, Extremwertstatistik, Windlastkollektive, numerische Simulation," DLR-Schlussbericht zum BMWi-Projekt, <https://doi.org/10.2314/KXP:1778971571>.
- [22] Pfahl, A., Buselmeier, M., Zschke, M., 2011. "Determination of Wind Loads on Heliostats," *Proc. SolarPACES 2011 Conference*, Granada.
- [23] Pfahl, A. and Dohmen, V., 2024. "Low-Cost Materials for Heliostats: Cost Comparison of Extensive or Moderate Use of Timber, Concrete, and Polymers," *SolarPACES Conference Proceedings*, 2, (Sep. 2024). DOI:<https://doi.org/10.52825/solarpaces.v2i.910>.
- [24] A.S. Pidaparthi, J.E. Hoffmann, 2017, "Effect of Heliostat Size on the levelized cost of electricity for power towers," *AIP Conference Proceedings* 1 (1850) 030038.
- [25] F. Von Reeken, G. Weinrebe, T. Keck, M. Balz, *Heliostat cost optimization study, SolarPACES (2015)*, 2015 conference.
- [26] Vásquez-Arango, J.F., 2016. "Dynamic Wind Loads on Heliostats," PhD Thesis, DLR, Uni Aachen, [https://elib.dlr.de/110613/1/Diss\\_Vasquez.pdf](https://elib.dlr.de/110613/1/Diss_Vasquez.pdf).
- [27] Z. Wu, B. Gong, Z. Wang, Z. Li, C. Zang, *An Experimental and numerical study of the gap effect on wind load on heliostat, Renew. Energy* 35 (2010) 797–806.
- [28] R. Zaibel, E. Dagan, J. Karni, H. Ries, *An Astigmatic corrected target-aligned heliostat for high concentration, Sol. Energy Mater. Sol. Cells* 37 (1995) 191–202, [https://doi.org/10.1016/0927-0248\(94\)00206-1](https://doi.org/10.1016/0927-0248(94)00206-1).